

# Structuring under Flow of Suspensions in a Gel

Laurent Jossic and Albert Magnin

Laboratoire de Rhéologie Domaine Universitaire, B.P. 53, 38041 Grenoble Cedex 9, France  
and

Université Joseph Fourier Grenoble 1, Institut National Polytechnique de Grenoble, CNRS UMR 5520, France

DOI 10.1002/aic.10219

Published online in Wiley InterScience (www.interscience.wiley.com).

*Laminar flow of a suspension of spheres in a gelled fluid through a sudden expansion causes the suspended matter to become organized. Segregation and migration phenomena of mono and bi-disperse suspensions have been highlighted. If different sizes of spheres and bimodal suspensions are used, this phenomenon can be used to form structured materials. Flow conditions are such that gravity effects and inertia are negligible. At rest, the spheres are stable in the gel. Nuclear magnetic resonance imaging was used to reveal the distribution of matter within the suspension downstream of the expansion. The interest of such structures for industrial applications is discussed. © 2004 American Institute of Chemical Engineers AIChE J, 50: 2691–2696, 2004*

**Keywords:** segregation, migration, gels, fluid mechanics, suspensions, rheology, NMRI

## Introduction

Particle suspensions in gelled fluids represent a widespread class of materials. The fluid suspending phase is often gelled in order to maintain in suspension and stabilize particles denser or lighter than the gel. The knowledge of the mechanics of suspensions in gelled fluids under flow is limited, particularly in the case of stability in flow conditions. The main reasons for this include first the lack of basic knowledge, for example, concerning the stability of isolated objects (Jossic and Magnin, 2001), and, second, the fact that analysis of these materials, which are usually opaque even at low-volume concentrations, calls for the use of modern imaging techniques (Fukushima, 1999). Lastly, the specific nature of viscoplasticity means that rheometric parameters, particularly slip (Magnin and Piau, 1987, 1990) must be carefully controlled if yield stresses are to be accurately measured.

By considering the inertialess flow of a suspension of mono-disperse spheres in a viscoplastic fluid through a sudden expansion, and by using nuclear magnetic resonance imaging (NMRI), Jossic et al. (2001) provided new basic knowledge of these phenomena. When the diameters of the upstream pipe and suspended spheres are of the same order of magnitude, the

solid matter becomes organized in the downstream pipe. The spheres form a concentrated ring provided the flow remains laminar. It should be pointed out that the suspensions used in this study are highly stabilized: in static conditions, the suspended spheres cannot move simply under the effect of gravity. Unlike the first study, restricted to one ratio diameter and a monodisperse suspension, this study considers different ratio diameters and bi-disperse suspensions.

The aim of this study is a better understanding of this phenomenon. The effect of ratio diameter between the upstream pipe and suspended spheres is investigated. A further topic of interest will be bimodal suspensions, by considering suspensions consisting of two populations of spheres.

To do this, the geometry of the expansion is presented first, along with an analysis of the resulting flow and the main features of the experimental setup and model suspensions. The NMRI protocol is then discussed. Images of the spatial distribution of the spheres within the suspension are used to evaluate the effects of the ratio of upstream pipe diameter to sphere diameter, volume concentration and the polydispersity of the structures formed downstream of the sudden expansion. Consequences and interest of these phenomena for industrial manufacturing process, and creation of new textures are discussed.

## Theoretical Approach

The behavior of the viscoplastic fluid forming the suspending phase can be modeled by a Herschel-Bulkley equation

Correspondence concerning this article should be addressed to L. Jossic at laurent.jossic@hmg.inpg.fr.

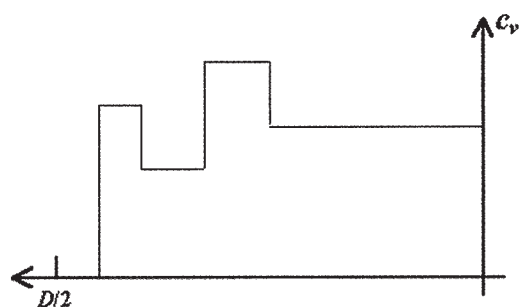


**Figure 1. Flow of a bimodal suspension in a sudden expansion and resultant theoretical concentration profile for a bimodal suspension  $\lambda=8$  and  $\lambda=4$ .**

$$\begin{cases} \tau = 2 \left( K \dot{\gamma}^{n-1} + \frac{\tau_0}{\dot{\gamma}} \right) \underline{D} & \text{if } \tau_{II} > \tau_0 \\ \underline{D} = 0 & \text{if } \tau_{II} \leq \tau_0 \end{cases} \quad (1)$$

with  $\tau_0$  being the yield stress,  $K$  the consistency,  $n$  the flow index,  $\underline{D}$  the rate of deformation tensor,  $\dot{\gamma}$  the second invariant of the rate of deformation tensor,  $\underline{\tau}$  the stress tensor deviator, and  $\tau_{II}$  the second invariant of the stress tensor deviator.

The flow configuration in the sudden expansion and the resulting theoretical concentration profile are represented in Figure 1. The flow is vertical, ascending and axisymmetric. The Reynolds number, the ratio of inertia effects to viscous effects, and the Oldroyd number, the ratio of yield stress effects to viscous effects, are expressed as follows

$$Re = \frac{\rho d^n U^{2-n}}{K} \quad (2)$$

$$Od = \frac{\tau_0}{K(U/d)^n} \quad (3)$$

$U$  is the flow rate velocity of the suspension in the upstream pipe and  $\rho$  is the gel density. The diameter of the pipe is designated  $d$ . The velocities and yield stresses were chosen in such a way that  $Re$  is small (no inertia effect) and  $Od$  is large (significant yield stress effects). The conditions thus favor the formation of organized structures during flow through the sudden expansion.

The sphere volume fraction  $c_v$  is the ratio of the volume occupied by the spheres to the total volume of the suspension. A further ratio used to describe the flow is  $\lambda = d/l$ , the ratio of the upstream pipe diameter to that of the spheres.

The ratio of yield stress effects to gravity effects is represented by

$$Y = \frac{\tau_0}{gl\Delta\rho} \quad (4)$$

$g$  designates gravity acceleration and the difference in density of the gel and spheres. In this study,  $Y$  is very much higher than the stability criterion, which is of the order of  $7.10^{-2}$  (Chhabra, 1993; Jossic and Magnin, 2001). This corresponds to the minimum value of  $Y$  beyond which an isolated sphere is kept in suspension.

The formation of the structures, for a monodisperse suspension, has been modeled by Jossic et al. (2001), based on a calculation of flow rate conservation. Indeed, it can be shown that a streamline passing through the region in the downstream pipe to which the spheres tend to migrate also passes through the spheres in contact with the wall of the upstream pipe. Considering a current tube with the diameter of the rings in the downstream pipe  $D_\lambda$  as its diameter, then its diameter in the upstream pipe  $d_\lambda$  is given by

$$\frac{d_\lambda}{d} = \frac{D_\lambda}{D} = 1 - \frac{1}{\lambda} \quad (5)$$

The probability of a given sphere being in contact with the pipe wall rather than in the vicinity of the center line is all the greater the closer the ratio of the upstream pipe diameter to the diameter of the sphere is to 1. As a first approximation, this probability may be estimated by calculating the ratio of the area of the nearby pipe to the additional area for a given section, respectively  $S_1$  and  $S_2$  on Figure 2. The nearby pipe is defined by a ring whose outer diameter is that of the pipe  $d$  and whose thickness is the diameter of a sphere  $l$ . Hence

$$R(\lambda) = 4 \frac{\lambda - 1}{(\lambda - 2)^2} \quad (6)$$

It should be noted that when  $\lambda$  tends toward 2,  $R(\lambda)$  tends toward infinity. In theory, therefore, all the spheres tend to gather only in the concentrated zone downstream of the expansion. Changes in  $D_\lambda/D$  and  $R$  as a function of  $\lambda$  are represented in Figure 3.

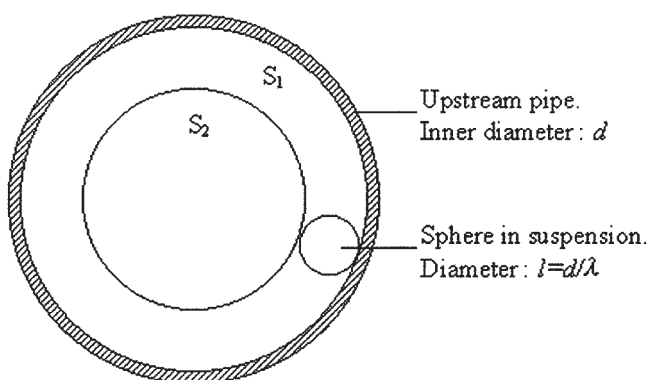


**Figure 2.** Representation of areas  $S_1$  and  $S_2$  used to calculate the probability for a given sphere being in contact with the pipe wall rather than in the vicinity of the center line.

## Experimental

The upstream pipe is supplied by the movement at controlled speed of a piston forming the reservoir. The flow rate velocity in the upstream pipe is kept constant and equal to  $0.7 \times 10^{-3} \text{ ms}^{-1}$ . This pipe consists of a transparent tube with an inner diameter  $d=4 \text{ mm}$ . The pressures exerted on the inside of this pipe during the various tests are insufficient to modify significantly the inner diameter. The pipe's length is  $25d$ . As inertia effects are low, flow development lengths are short. The sudden expansion was obtained by connecting the upstream pipe to a cylinder of inner diameter  $D=42 \text{ mm}$ . This cylinder is made of transparent Plexiglas or made of PVC. The cylinder is  $4 \text{ cm}$  long.

The suspension was made to flow close to the NMR core. The downstream pipe was then placed in the antenna, which is positioned in the NMR core. The images are thus obtained in static conditions. Initially, the upstream and downstream pipes are empty and are then filled progressively. There is, thus, a transient phase of flow before steady conditions are achieved. These steady conditions are obtained when the unconfined surface is far from the expansion.

Carbopol® 940 resin made by Goodrich was used to obtain

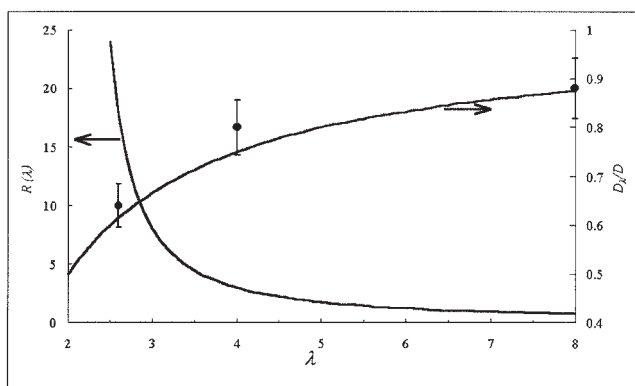


**Figure 3.** Theoretical and experimental changes in the diameter of concentrated zones in the downstream pipe as a function of the probability of a sphere being in contact with the wall of the upstream pipe.

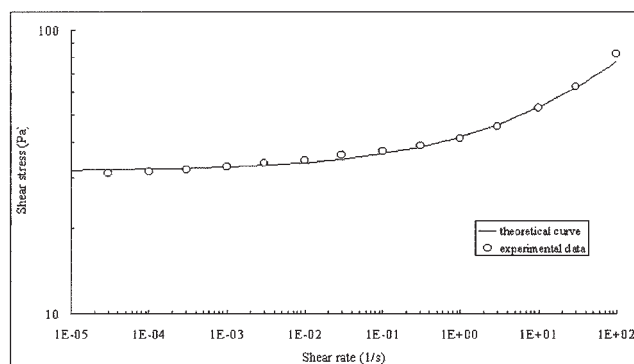


**Figure 4.** Flow curve for Carbopol gel.  $c_m=0.15\%$ .

a transparent aqueous gel. The gel is made by mixing the polymer in water. During neutralization by adding NaOH, the gel becomes viscoplastic. The yield stress value can be adjusted according to the mass concentration  $c_m$  and the pH. The material obtained in this way is viscoplastic and nonthixotropic (Magnin and Piau, 1987, 1990); its properties are stable over time. The mass fraction of the gel used in this study was  $c_m=0.15\%$ . The yield stress was finely characterized by controlled speed rotating rheometry in a cone-plate cell, using a Carrimed Weissenberg rheogoniometer. Evaporation and wall-slip effects were monitored (Magnin and Piau, 1987, 1990). Figure 4 represents the changes in shear stress as a function of shear rate in steady conditions. The curve was modeled by a Herschel-Bulkley law (Eq. 1) with the following parameters:  $\tau_0 = 32 \text{ Pa}$ ,  $K = 10 \text{ Pa} \cdot \text{s}^{-0.32}$ ,  $n = 0.32$ .

Polystyrene spheres made by Marseille Chimie Berre l'Etang were used in the experiment. They have a density of  $\rho=1060 \text{ kg} \cdot \text{m}^{-3}$ . Three sets of spheres with dia.  $l=0.5 \pm 0.05 \text{ mm}$ ,  $l=1 \pm 0.05 \text{ mm}$  and  $l=1.5 \pm 0.05 \text{ mm}$ , that is,  $\lambda=8$ ,  $\lambda=4$ ,  $\lambda=2.6$ , respectively, were obtained by sieving. Little water, of the order of 1%, is absorbed by the spheres. The sphere diameter, thus, varies very little when they are in suspension in the aqueous phase.

The gel and spheres were mixed directly in the supply reservoir. A mixer adapted to the dimensions of the reservoir and to viscoplastic fluids was developed. The homogeneity of the reservoir contents was checked visually, and by NMRI observations.

NMR images were obtained at the NMR Laboratory of the CPE Lyon (Claude Bernard University). The NMR core magnet used a horizontal Oxford superconductor with an intensity of  $2 \text{ T}$ . The meridian plane images resolution is  $468 \mu\text{m}$ , and the horizontal cross-section images resolution is  $180 \mu\text{m}$ . As the gel is highly aqueous, and the suspended spheres are made of polystyrene, the signal-to-noise ratio is high, it gives well contrasted images. More information about the NMR technique was given by Jossic et al. (2001).

The NIH software has been used to illustrate the distribution of matter in the downstream pipe. This software, based on pixel intensity integration was described by Jossic et al. (2001).

## Observations

The first point considered is the effect of diameters ratio  $\lambda=l/d$  on the structures formed with  $\lambda=8$ ,  $\lambda=4$  and  $\lambda=2.6$ , and a volume concentration  $c_v=5\%$ . These values of  $\lambda$  correspond

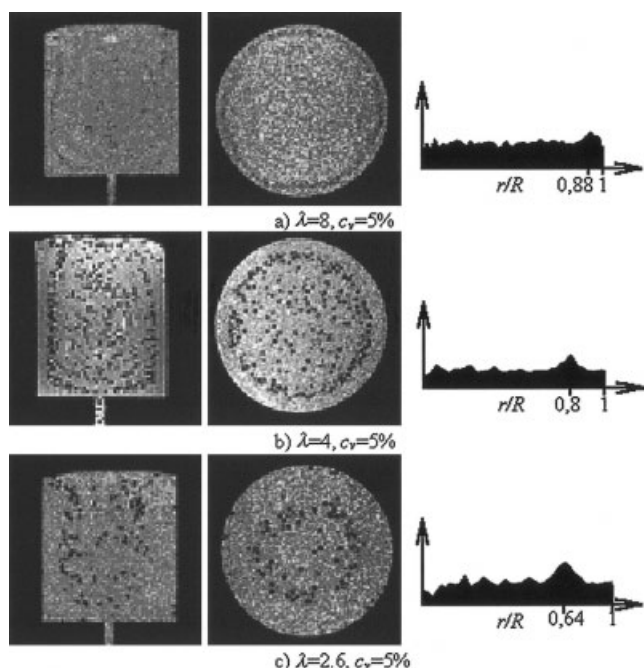


**Figure 5. Structures formed as a function of ratio diameters  $\lambda$ . ( $c_v=5\%$ ,  $\lambda=8$ ,  $\lambda=4$ ,  $\lambda=2.6$ ).**

For each  $\lambda$ , from left to right, meridian plane, horizontal section and concentration profile from the pipe axis to the inner surface.

to very significant wall effects and are representative of a noncontinuous medium. The second point considered is the effect of the volume fraction, with  $c_v=20\%$  for  $\lambda=8$  and  $\lambda=4$ . Third, the structure of two bimodal suspensions is analyzed; these consist of two populations of spheres,  $\lambda=8$  and  $\lambda=2.6$  then  $\lambda=8$  and  $\lambda=4$  for total volume concentrations of  $c_v=10\%$ .

### Flow conditions

The yield stress of the gel is  $\tau_0 = 32$  Pa, and the difference in density is  $60 \text{ kg.m}^{-3}$ . Three populations of spheres with diameters of  $l=0.5$  mm,  $l=1$  mm and  $l=1.5$  mm were used. According to Eq. 4, these numerical values give  $Y=108$ ,  $Y=54$  and  $Y=27$ , respectively. These values, which are very much higher than the stability criterion, show that the suspensions are highly gelled and that at rest the spheres are firmly stabilized by the gel.

Before presenting the results later, it is important to point out that the images showed that the spheres were distributed regularly in the upstream pipe, with no segregation or particular structure of the suspension being observed there. Due to low inertia effects and high plasticity effects, no vortex appears in the downstream pipe, (Jay et al., 2001).

### Effect of diameters ratio $\lambda$

Figure 5 shows the structures obtained with suspensions such that  $\lambda=8$ ,  $\lambda=4$  and  $\lambda=2.6$ , each with a concentration of  $c_v=5\%$ . The pairs  $(Re, Od)$ , Eqs. 2 and 3, upstream and downstream of the sudden expansion have values of, respectively  $(10^{-4}, 7)$ , and  $(2 \times 10^{-7}, 75)$ . These last two values were obtained by taking the downstream pipe diameter as the length scale, and the velocity in the downstream pipe as the velocity

scale. The images show the spatial distribution of the spheres in these flow conditions.

Let us consider first, the case of  $\lambda=4$  (Figure 5b) and examine the image of the meridian plane from top to bottom:

- Due to transient filling conditions and the presence of the unconfined surface, the structure of the suspension in the upper part of the downstream pipe is disturbed.
- The region situated below these disturbances corresponds to the established flow conditions. The distribution of solid matter is structured. This zone clearly appears on the image of the horizontal section.
- At the expansion, there is no sphere in the vicinity of the right angle, which corresponds to a rigid static zone where there is no flow. It is produced by the presence of the yield stress (Jay et al., 2001; Hammad et al., 1999; Vradis et al., 1997). At the entrance to the downstream pipe, a flow expansion zone is formed. This may be described by a development length of the order of  $2d$ .

The image of a representative horizontal section taken in the developed flow zone provides the following information:

- Very few spheres are located near the walls. Indeed, with a constant thickness of the order of several sphere diameters, the volume concentration is of the order of zero. The thickness  $e$  can be estimated by

$$\frac{e}{D} = \frac{1}{2\lambda} \quad (7)$$

- The second region is more concentrated and forms a cylinder whose center line is the same as that of the pipe. The mean diameter of this cylinder is of the order of 34 mm, that is,  $D_4/D=0.8$ . The graph in Figure 3 shows that Eq. 5 of the model correctly predicts the diameter of the concentrated zone downstream of the expansion. The thickness of the concentrated zone is of the order of two to three sphere diameters. The spheres are in contact with one another in this zone. The volume concentration is, therefore, greater than the mean volume concentration of the suspension, which is 5%.

- The third region is the central zone of the cylinder referred to earlier. The mean volume fraction here is very much lower than the mean concentration.

According to Eq. 6, for  $\lambda=4$ , it is three times as likely that a sphere will be in contact with the wall than in the vicinity of the pipe center line. Statistically, therefore, 75% of spheres in the upstream pipe are situated in the vicinity of the wall and, hence, in the ring of dia.  $D_4$  downstream of the expansion, and 25% in the vicinity of the center line. The image of the horizontal section shows that the sphere distribution between the concentrated zone of dia.  $D_4$  and the central zone is generally speaking of the same order of magnitude.

Let us now consider the cases  $\lambda=8$  and  $\lambda=2.6$ , shown in Figure 5a and 5c, respectively. The structures are similar to the one just described. Only the mean diameter of the concentrated zone differs from one case to another. It increases when the diameter of the suspended spheres decreases. According to the images of the horizontal sections,  $D_8/D \approx 0.88$  and  $D_{2.6}/D \approx 0.64$  (Figure 5). Figure 3 shows that these values validate the model Eqs. 5 and 7.

The concentration profiles illustrate the decrease in diameter of the concentrated zone when the sphere diameter increases.



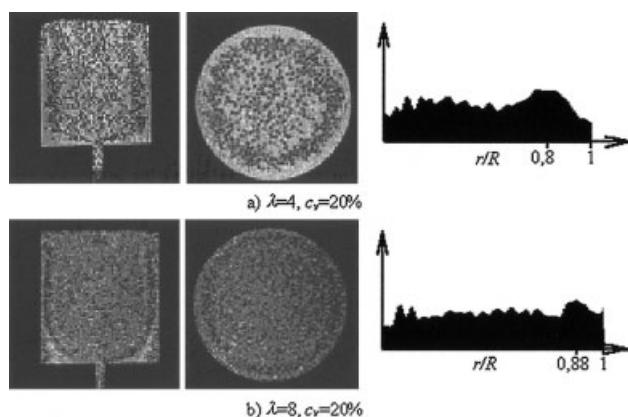


**Figure 6. Structures formed with a concentrated suspensions. ( $c_v=20\%$ ,  $\lambda=8$ ,  $\lambda=4$ ).**

For each  $\lambda$ , from left to right, meridian plane, horizontal section and concentration profile from the pipe axis to the inner surface.

Additionally, they reveal a more or less constant concentration along the radius, outside the concentrated zone.

It is important to point out that for  $\lambda=8$  and  $c_v=5\%$  the suspension is opaque, whereas for  $\lambda=2.6$  and  $c_v=5\%$  it is not. This can be seen on the images where  $\lambda=8$ , by the fact that in the region close to the pipe center line, which in theory has a low concentration, there are in fact many spheres. However, they are not close enough to one another to form a zone that is sufficiently concentrated to appear in the image. In addition, the resolution is too low to be able to distinguish the spheres from one another. If the suspension is observed with the naked eye, it is impossible to discern any region that is more concentrated than the others, indicating that the spheres are in theory distributed uniformly throughout the volume of the lower pipe, which is contradicted by the NMR images.

### Concentrated suspensions

Let us consider now the structures obtained with concentrations of  $c_v=20\%$  such that  $\lambda=8$  and  $\lambda=4$  (Figure 6). These structures are similar to those revealed in the case of monodisperse suspensions with 5% concentrations.

Let us consider first of all the case  $\lambda=4$  (Figure 6a). The image of the meridian plane, described from top to bottom, illustrates the following points:

- The disturbances due to the free surface and transient conditions extend over a much greater length scale than in the case of  $c_v=5\%$ , they tend to homogenize the spatial distribution of the spheres near the free surface.
- The distribution of solid matter in the developed conditions domain is similar to that observed previously, but is more diffuse. The boundary between the concentrated zone and central zone is much less clearly defined.
- The rigid static zone appears to be less extensive than for  $c_v=5\%$ .

The image of the horizontal section completes the image of the meridian plane.

- The wall area, which has very little solid matter, is more or less of the same thickness as in the case of  $c_v=5\%$ .
- The shape of the concentrated zone is always cylindrical

and coaxial with the pipe. The thickness of this concentrated zone in this case is of the order of about 10 sphere dia.. The mean diameter is still of the order of  $D_4 \approx 34$  mm.

- The volume concentration of the central zone is less than the mean volume concentration of the suspension.

The images obtained for  $\lambda=8$  (Figure 6b) do not show any obvious difference with regard to the geometry of the structure formed by the spheres. As with  $c_v=5\%$ , the main difference in comparison with the case of  $\lambda=4$  is the diameter of the concentrated zone. The value obtained for  $D_8$ , when  $c_v=20\%$ , is still of the order of 37 mm, the value obtained when  $c_v=5\%$ .

The concentration profiles clearly illustrate the expansion of the concentrated zone. They confirm that the diameters of the concentrated zones for these two suspensions are the same as for  $c_v=5\%$ . The concentration peaks are indeed situated more or less on the same radius as on Figure 5.

### Bimodal suspensions

The images obtained for two polydisperse suspensions are represented on Figure 7. These mixtures are defined by ( $\lambda=8$ ,  $c_v=5\%$ ;  $\lambda=2.6$ ,  $c_v=5\%$ ) and ( $\lambda=8$ ,  $c_v=5\%$ ;  $\lambda=4$ ,  $c_v=5\%$ ). The mixture ( $\lambda=8$ ,  $c_v=5\%$ ;  $\lambda=2.6$ ,  $c_v=5\%$ ), Figure 7a, for which the images are the most contrasted, will be analyzed first.

The image of the meridian plane shows that the spheres are segregated according to their diameter.

- At the free surface, disturbances linked with the transient conditions are not very extensive.
- In the region of developed flow, the spheres segregate according to size. From the wall of the downstream pipe to the vertical center line, several successive concentration domains are formed. Near the wall, the small diameter spheres ( $\lambda=8$ ) form an initial highly concentrated zone. Then, there is a less concentrated zone, bounded by a region with a high concentration of large spheres ( $\lambda=2.6$ ). The vicinity of the center line is once again less concentrated. Nevertheless, given the small diameter of the spheres ( $\lambda=8$ ), this does not mean that this region is lacking in spheres, for the reasons outlined earlier.
- In the lower part of the downstream pipe, the expansion of

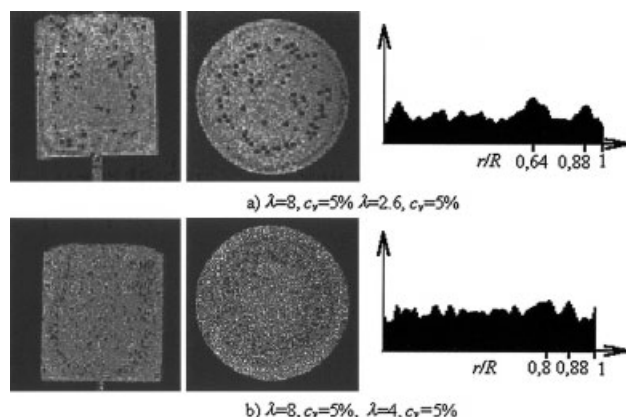


**Figure 7. Structures formed in bimodal suspensions. ( $\lambda=8$ ,  $c_v=5\%$ ;  $\lambda=2.6$ ,  $c_v=5\%$ ) and ( $\lambda=8$ ,  $c_v=5\%$ ;  $\lambda=4$ ,  $c_v=5\%$ ).**

For each concentration, from left to right, meridian plane, horizontal section and concentration profile from the pipe axis to the inner surface.

the concentrated zones depends on the sphere diameter. The small diameter spheres follow the bottom of the downstream pipe, subsequently propagating along the static rigid zone and then along the walls. The large spheres ( $\lambda=2.6$ ) follow a vertical track more rapidly.

The concentration profiles confirm the previous observations. They indeed show that there are two concentration peaks.

The rings observed previously (Figure 5a and 5c) are superimposed in the horizontal section.

- Near the wall, the small diameter spheres ( $\lambda=8$ ) form an initial circular concentrated zone. The diameter of the ring ( $D_8 \approx 37$  mm) is identical to that obtained in the case of the monodisperse suspension.

- A second concentrated zone is formed with the large diameter spheres ( $\lambda=2.6$ ). The mean diameter of this zone ( $D_{2.6} \approx 27$  mm) is similar to that obtained in the case of the monodisperse suspension. As a consequence, segregation of different particle sizes in a bimodal suspension can be predicted with Eq. 5.

The zone bounded by these two regions, like the central zone of the downstream pipe, seems to have a low concentration. Nevertheless, observation of the downstream pipe with the naked eye shows that there is a relatively large number of small diameter spheres ( $\lambda=8$ ) in these regions. These spheres do not appear on the images for the reasons outlined earlier.

Although there is little contrast, the images obtained with the ( $\lambda=8$ ,  $c_v=5\%$ ;  $\lambda=4$ ,  $c_v=5\%$ ) mixture (Figure 7b) suggest that the distribution of matter is quite similar. The phenomenon is less marked, as the rings formed in the horizontal sections have diameters of the same order of magnitude and, therefore, tend to be superimposed. Nevertheless, it is still possible to conclude that the spheres are segregated according to their diameter.

## Conclusions

This study demonstrates that laminar flows of homogeneous suspensions in a sudden expansion undergo migration and segregation of suspended particles that can be used to create organized structures. Indeed, the observed structures for suspensions of sphere in a gelled fluid are interesting for industrial applications. Let us remember that at rest, these suspensions are strongly stabilized by the yield stress of the fluid suspending phase. Before flow starts, particles in suspension are randomly dispatched. Such a complex flow field as one in an expansion gives rise to particles migrations and segregations. The shapes of the resulting structures are a function of the polydispersity of the suspension and diameters ratio. Those structures were clearly revealed by NMRI.

The studied configurations correspond to industrial setup such as the filling of tanks with, for example, food suspension. The tanks filled this way, present an organized structure. This situation can be prejudicial for the homogeneity of the product when the tank is emptied.

Second, the gelling property of the suspending phase can be used so as to obtain materials with a controlled texture. During the extrusion of such suspensions, no sphere appears on the surface of the exudates. The surface is smooth. Products with aesthetic constraint could be manufactured this way. In addition,

the solid matter in suspension can be used as a mechanical reinforcement, but also, if the particles in suspension are metallic, as an electric conductor. Food process applications could also be found for products with particular textures. The suspending gel allows the suspension stability for high volume fractions of particles to be maintained.

## Notation

$d$  = diameter of upstream pipe, m  
 $D$  = diameter of downstream pipe, m  
 $\dot{D}$  = rate of deformation tensor,  $s^{-1}$   
 $g$  = gravity,  $m.s^{-2}$   
 $K$  = consistency,  $Pa.s^n$   
 $l$  = diameter of spheres, m  
 $R$  = radius, m  
 $U$  = upstream flow rate velocity,  $m.s^{-1}$   
 $u$  = downstream flow rate velocity,  $m.s^{-1}$

## Greek letters

$\tau_0$  = yield stress (Pa).  
 $\tau$  = stress tensor deviator, Pa  
 $\tau_{II}$  = second invariant of the stress tensor deviator (Pa)  
 $\dot{\gamma}$  = second invariant of the rate of deformation tensor,  $s^{-1}$   
 $\rho$  = density,  $kg.m^{-3}$   
 $\Delta\rho$  = difference in density between fluid and spheres,  $kg.m^{-3}$

## Dimensionless numbers

$\lambda = l/d$  = ratio of diameters  
 $Od = \tau_0/K(U/d)^n$  = Oldroyd number.  
 $c_v$  = volume fraction.  
 $n$  = flow index.  
 $Re = \rho U^{2-n} d^n / K$   
 = Reynolds number.  
 $Y = \tau_0/g/\Delta\rho$  = ratio of yield stress effects to gravity effects.

## Acknowledgment

The authors wish to thanks Professor Briguët, Director of the CPE Lyon NMR laboratory, and Linda Chaabane and Rachid Mahdjoub for their valuable contribution to the NMR experiments.

## Literature Cited

- Chhabra, R. P., *Bubbles, Drops and Particles in Non-Newtonian Fluids*, CRC Press (1993).  
 Fukushima, E., "Nuclear Magnetic Resonance as a Tool to Study Flow," *Annu. Rev. Fluid Mech.*, **31**, 95 (1999).  
 Hammad, K. J., M. V. Ötügen, G. C. Vradis, and E. B. Arik, "Laminar Flow of a Nonlinear Viscoplastic Fluid Through an Axisymmetric Sudden Expansion," *J. of Fluids Eng.*, **121**, 488 (1999).  
 Jay P., A. Magnin, and J.-M., Piau, "Viscoplastic Flow Through a Sudden Expansion," *AIChE J.*, **47** (10), 2155 (2001).  
 Jossic, L., A. Briguët, and A. Magnin, "Segregation under Flow of Objects Suspended in a Yield Stress Fluid and NMR Imaging Visualisation," *Chem. Eng. Sci.*, **57**, 409 (2001).  
 Jossic, L., and A. Magnin, "Drag and Stability of Objects in a Yield Stress Fluid," *AIChE J.*, **47** (12), 2666 (2001).  
 Magnin, A., and J. M. Piau, "Shear rheometry of Fluids with a Yield Stress," *J. Non-Newtonian Fluid Mech.*, **23**, 91 (1987).  
 Magnin, A., and J. M. Piau, "Cone and Plate Rheometry of Yield Stress Fluids. Study of an Aqueous Gel," *J. Non-Newtonian Fluid Mech.*, **36**, 85 (1990).  
 Vradis, G. C., and M. V. Ötügen, "The Axisymmetric Sudden Expansion Flow of a Non-Newtonian Viscoplastic Fluid," *J. of Fluids Eng.*, **119**, 193 (1997).

Manuscript received Aug. 27, 2003, and revision received Mar. 11, 2004.